JOURNAL OF MATERIALS SCIENCE 33 (1998) 1369–1377

Synthesis of ditungsten carbide by controlled decomposition of $Cp_2W_2(CO)_4$ (dmad) under a hydrogen atmosphere

J.-M. GIRAUDON, P. DEVASSINE, L. LECLERCQ, G. LECLERCQ
Laboratoire de Catalyse Hétérogène et Homogène, URA CNRS no. 402, Université des Sciences et Technologies de Lille, 59655 Villeneuve d'Ascq Cédex, France

Controlled decomposition studies of the *bis*(cyclopentadienyl)ditungsten(tetracarbonyl)-dimethylacetylenedicarboxylate ($Cp_2W_2(CO)_4$(dmad)) under flowing hydrogen show that it totally decomposes at 600 °C for 2 h to give a pure bulk W_2C as revealed by X-ray diffraction. Excess oxygen and carbon at the surface are detected by X-ray photoelectron spectroscopy. An *in situ* temperature-programmed X-ray diffraction experiment performed on $Cp_2W_2(CO)_4$ (dmad) shows the detection temperature of W_2C to be 600 °C, the sample being amorphous or microcrystalline below that temperature. Based on previous results obtained for the decomposition of $Cp_2Mo_2(CO)_4$(dmad) on the one hand, and thermogravimetric and chromatographic analyses performed on $Cp_2W_2(CO)_4$ (dmad), on the other, a decomposition scheme of the latter under hydrogen has been proposed. © *1998 Chapman & Hall*

1. Introduction

A number of studies have shown that organometallic compounds can be used as precursors to generate refractory metal materials. In particular, different strategies have been undertaken to generate such materials in the field of carbides of group VI transition metals, especially for tungsten, i.e. WC and W_2C [1–4]. These solids are well known for having properties such as hardness, corrosion resistance and thermal stability, which make them useful materials for protective coating applications [5].

Thus, a chemical vapour deposition approach can be used. A prerequisite for such a method is that the organometallic precursors will volatilize easily and thermolyse at low temperature. Moreover, hydrogen and carbon must be the only elements in the ligands in order to avoid heteroatoms contamination. A clear illustration of this is the production of WC thin film from the carbyne complex $(Me_3CCH_2)_3W{\equiv}CCMe_3$ reported by Xue *et al.* [3]. Another strategy is the pyrolysis of organometallic complexes so that only one non-metallic element, here carbon, will remain bound to the metal during such a decomposition. This conceptual approach has been put forward by Laine and Hirschon [1]. From that point of view, the premetallic must be polynuclear, a strong interaction between the metal and the carbon being desirable. Furthermore, oxygen–metal or halogen–metal bonds should be avoided to prevent incorporation of these elements in the material. To validate their concepts, Laine and Hirschon have demonstrated that bis(cyclopentadienyl)ditungsten(tetracarbonyl)-dimethylacetylenedicarboxylate ($Cp_2W_2(CO)_4$(dmad)) (Fig. 1), in which the bonding arrangement involves two tungsten atoms and two carbons in a tetrahedral arrangement, decomposed at about 700 °C in nitrogen to give good yields of W_2C. However, traces of WO_2 have been detected by X-ray diffraction (XRD) and excess carbon has also been observed as a by-product.

It is noteworthy that both pyrolysis conditions and the choice of the precursor can affect the product selectivities.

Based on the results obtained by Laine and Hirschon [1], we have undertaken the decomposition of this precursor in hydrogen in order to try and avoid the formation of tungsten oxides. Such a procedure has been previously employed in our laboratory with success in the case of the molybdenum homologue compound of $Cp_2W_2(CO)_4$(dmad), i.e. $Cp_2MO_2(CO)_4$(dmad) [6].

2. Experimental procedure

2.1. Synthesis

The preparation of the organometallic species was carried out in a dry and oxygen-free argon atmosphere using standard Schlenk techniques. Solvents (tetrahydrofuran (THF), ether) were dried by distillation from sodium-benzophenone except for hexane, which was distilled on calcium hydride. They were thoroughly deoxygenated before use.

$W(CO)_6$ and $H_3CCO_2{-}C{\equiv}C{-}CO_2CH_3$ were purchased from Aldrich and used without further purification. $CpW(CO)_3H$ was prepared according to the procedure described elsewhere [7].

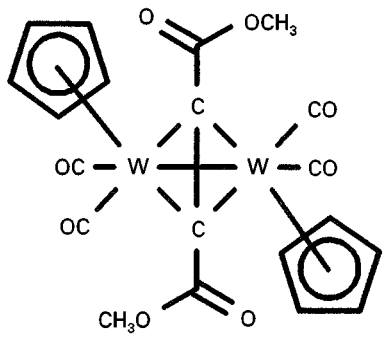

Figure 1 Representation of $Cp_2W_2(CO)_4$(dmad).

2.1.1. $Cp_2W_2(CO)_4$(dmad)

This compound was synthesized according to the route established by Laine and Ford [8]. Dimethylacetylenedicarboxylate (860 mg) was added with a syringe to a stirred solution of $CpW(CO)_3H$ (300 mg = 8.99×10^{-4} mol) in tetrahydrofuran (THF; 30 ml). After one night at reflux of THF, the solvent was evaporated under vacuum and the residue was pumped overnight to remove any excess dimethylacetylenedicarboxylate. The solid was dissolved in a minimum of CH_2Cl_2 and was chromatographed on a silica gel column. Elution with 10% ether/hexane mixture allowed the recovery of an orange powder (50 mg).

Recrystallization from ether yielded red crystals. Data for the tungsten complex are as follows:
anal. calc. for $W_2C_{20}H_{16}O_8$: C, 3.19; H, 2.14, found C, 3.19; H, 2.8.
IR (KBr, cm^{-1}): 2009, 2001, 1974, 1958, 1937, 1918, 1854, 1863.
^1H NMR ($CDCl_3$): 5.38 (10 H, s, Cp); 3.74 (6H, s, –OMe).

2.1.2. W_2C

The decomposition of $Cp_2W_2(CO)_4$(dmad) was performed by placing an amount of a few tenths of a milligram of the latter in a stainless steel boat, which was introduced into a quartz flow reactor fitted in a vertical furnace. After purging the apparatus in flowing nitrogen (30 min, 3 l h^{-1}), the decomposition was carried out in hydrogen at a flow rate of about 3.0 l h^{-1}. The temperature was increased at a rate of 100 °C h^{-1} from room temperature to a final value of 600 or 830 °C. The final temperature was maintained for 2 h (600 °C) or 1 h (830 °C). Then the reactor was allowed to cool to room temperature in hydrogen. At room temperature, the hydrogen flow was stopped and replaced by flowing nitrogen. Then the materials were passivated in a flow of 2% O_2N_2 mixture (2 l h^{-1}) for 6 h.

The composition of the gas mixture at the outlet of the reactor during the decomposition of $Cp_2W_2(CO)_4$(dmad), carried out in accordance with the experimental procedure followed for WC600, except the duration of the isotherm, which was 1 h, was periodically measured by gas chromatography using a chromatograph HP 5910 A equipped with a thermal conductivity detector (TCD). Products were separated at 170 °C in a column (6 in long and 1/8 in wide; in $\sim 15.25\,cm \times 0.32\,cm$) filled with carbosphere molecular sieve. Peak areas were measured with an Intersmat ICR1 integrator. The material passivated in milder conditions as above, i.e. 0.2% O_2/N_2 for 4 h gives a pure W_2C by XRD.

2.2. Physical measurements

Elemental analyses were performed by the Service Central de Microanalyse du CNRS, Vernaison, France.

IR spectra were run using a Nicolet-Folder 510 TF apparatus with KBr pellets.

The bulk structure of the materials was determined by X-ray diffraction using either a Philips (Norelco PW 1051) apparatus (CuK_α radiation, $\lambda = 0.154\,178$ nm, nickel filter) or a diffractometer (Siemens 5000). The *in situ* temperature-programmed X-ray measurements were performed in a diffractometer Siemens D 500 equipped with a HTK 10 ANTOON PAAR high-temperature chamber and a fast linear counter: ELPHYSE. For such measurements, a few milligrams of $Cp_2W_2(CO)_4$(dmad) were not directly deposited as usual on the platinum cell, but on a gold plate. Such a procedure allowed us to protect the platinum cell from adventituous contamination during the melting step of $Cp_2W_2(CO)_4$(dmad).

The sample was submitted to a flow of 3 l h^{-1} hydrogen (quality U) from 27–900 °C with a heating rate of 102 °C h^{-1}. The diffraction patterns were recorded every hour. XRD patterns were assigned using the Joint Committee on Powder Standards (JCPDS) data base. The average size of the crystallites, D_c, was estimated from the Scherrer equation, $D_c = K\lambda/(\beta \cos\theta)$, where λ represents the X-ray wavelength, θ the Bragg angle, and β the full-width at half-maximum (FWHM) of the peak corrected for instrumental broadening. The constant K was taken to be 1.

XPS measurements were carried out with an AEI ES 200 B spectrophotometer equipped with an aluminium anode ($h\nu = 1486.6$ eV). The binding energies were determined by using the *in situ* $W4f_{5/2}$ peak of WO_3 at 38.2 ($\pm$0.2 eV) as reference. The choice of such a reference appears legitimate because this peak arising at the high binding energy end of the spectrum is poorly perturbated by the other photoelectron peaks arising from lower valence state forms of tungsten. From a WO_3 reference sample, the $W\,4f_{5/2}/W\,4f_{7/2}$ and the W satellite/$W\,4f_{7/2}$ area ratios were extracted, having ratios of 0.79 and 0.15. The separation between the $W\,4f_{7/2}$ and $W\,4f_{5/2}$ was set at 2.1 eV and the width ratio $W\,4f_{5/2}/W\,4f_{7/2}$ was assumed to be unity. The background was removed using a non-linear base-line correction, and spectral smoothing was carried out using the least squares method. All tungsten peaks were fitted using a Gaussian function. The relative distribution of the observed carbon components was resolved using a Gaussian fit function and a FWHM of 1.7 eV.

The surface atomic composition, n_a/n_b, was calculated using the equation [9]

$$n_a/n_b = I_a/I_b(\sigma_b/\sigma_a)(E_b/E_a)^{1.7} \quad (1)$$

where n_a/n_b is the atomic ratio between the elements A and B, I_a and I_b are the photoelectron peak areas, σ_a and σ_b are the cross-sections, E is the kinetic energy corresponding to the level under consideration.

The thermogravimetric analyses (TGA) were performed with a Sartorius Gmb H vacuum microbalance instrument in a flow of hydrogen ($3\,l\,h^{-1}$). The heating rate was $100\,^{\circ}C\,h^{-1}$ and the sample weights in the range of 10 mg. Prior to this treatment, the sample was purged under a flow of nitrogen ($3\,l\,h^{-1}$) at 115 °C.

3. Results and discussion

With the aim of obtaining tungsten dicarbide at the lowest possible temperature, a thermoreduction of $Cp_2W_2(CO)_4$(dmad) was realized and followed by thermogravimetric analysis. The TGA profile and the derivative curve for $Cp_2W_2(CO)_4$(dmad) in a hydrogen atmosphere are shown in Fig. 2a. The derivative curve broadly shows three peaks corresponding to the successive removal of the ligands linked to the metal. Neglecting the weight loss obtained before 100 °C probably due to the elimination of solvents of recrystallization, a total weight loss of 51.4% is obtained at 900 °C which corresponds approximately to the formation of tungsten metal (theoretical calculation = 51.1% weight loss i.e. an error of 0.6%). Keeping the isotherm for 10 h does not change the weight loss.

It must be pointed out that from a temperature of 550 °C, which represents the final temperature of the third peak, the weight loss is low (1.6%) and linear according to the temperature. This obtained value perfectly corresponds to that calculated (1.597%) for the transformation of W_2C into tungsten metal. The final compound has been passivated in a 2% O_2/N_2 mixture for 6 h ($2\,l\,h^{-1}$). The XRD diagram gives, in the 15–18 2θ window, three lines at 40.2°, 58.23° and 73.19°, which confirm the presence of tungsten metal.

Taking these results into account, two samples of $Cp_2W_2(CO)_4$(dmad), designated WC600 and WC830, have been decomposed in flowing hydrogen at 600 °C for 2 h and at 830 °C for 1 h, respectively. The samples were also submitted to a passivation step under 2% O_2/N_2 ($2\,l\,h^{-1}$) for 6 h before being contacted with air. In both cases, a grey powder was obtained (yield ≈ 70%). It is noteworthy that black residues condensed on the walls of the quartz tube. The X-ray diffraction pattern indicates the presence of pure W_2C in the sample treated at 600 °C (Table I). On the other hand, for the sample treated at 830 °C, in addition to the tungsten dicarbide lines, those characteristics of tungsten metal (Table I) can also be detected. The height ratio of the more intense lines of each of the two samples h_{W2C}/h_W is about 2.9.

To obtain more information concerning the surface composition of these two samples, XPS measurements

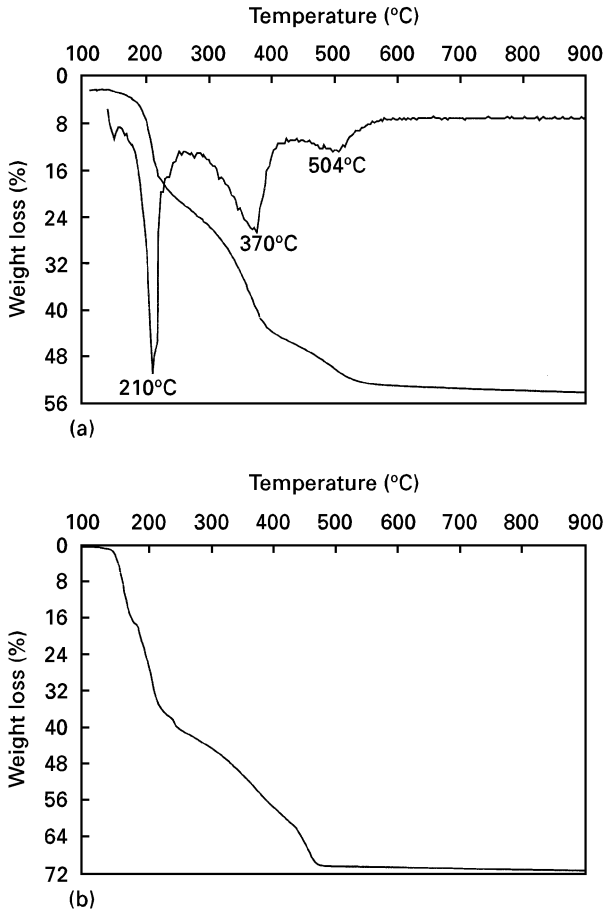

Figure 2 TGA profiles of the organometallic (a) tungsten and (b) molybdenum precursor (H_2; $3\,l\,h^{-1}$, $100\,^{\circ}C\,h^{-1}$).

TABLE I X-ray data for W_2C carbide

WC600		WC830		W_2C reference			W reference		
d_{exp}	I/I_o[a]	d_{exp} (nm)	I/I_o[a]	d_{th} (nm)	I/I_o	$h\,k\,l$	d_{th} (nm)	I/I_o	$h\,k\,l$
2.599	m	2.605	m	2.596	25	100			
2.368	m	2.365	m	2.364	22	002			
2.277	S	2.266	S	2.276	100	101			
		2.238	S				2.238	100	110
1.75	m	1.750	m	1.748	17	102			
		1.581	s				1.582	15	200
1.501	m	1.502	m	1.499	14	110			
1.347	m	1.348	m	1.347	14	103			

[a]S, strong; m, medium; s, small.

were carried out. Fig. 3 shows the photoelectron peaks of the W 4f core level for these two solids. At that stage it is worth mentioning that a small, high, binding energy peak appears at $+5.8 \pm 0.2$ eV, higher than the W $4f_{7/2}$ peak. This small, broad, peak was previously assigned to the W $5p_{3/2}$ level [10], yet recent studies have discarded such an attribution and have assimilated this photoelectron peak to a satellite [11]. At first sight, the spectrum of the sample decomposed at 600 °C (Fig. 3a) can be viewed as two sets of doublets. The one which peaks at 32.1 eV (W $4f_{7/2}$) and 34.2 eV (W $4f_{5/2}$) readily identifies a carbidic phase. The other one corresponds to the tungsten oxide species W^{6+} (at 36.1 and 38.2 eV). However, a closer examination of the carbidic doublet shows that the ratio of the heights of W $4f_{5/2}$ and W $4f_{7/2}$ is significantly greater than the multiplicity factor (0.95 compared to the theoretical ratio value of 0.75) and makes it possible to figure the existence of another tungsten species. Indeed, removal of the W 4f and of the satellite of the carbidic contribution from the global W 4f envelope reveals, besides the expected W^{6+} oxidic phase, a weak W $4f_{7/2}$ component at 34.4 eV agreeing with a W^{4+} species [12]. This peak overlaps with the W $4f_{5/2}$ peak of W_2C. Hence in the layer analysed by XPS, tungsten carbide exists with a mixture of oxide species.

Similarly, the W 4f peaks of the sample decomposed at 830 °C (Fig. 3b) roughly exhibit two doublets: one characteristic of the W^{6+} phase, the other of a reduced one denoted as $W^{(0)}$. As opposed to the previous one, the W $4f_{7/2}$ peak of the W^{6+} component is better separated, which in turn means that the reduced component is shifted towards weaker binding energies. Indeed the difference between the W $4f_{5/2}$ (W^{6+}) and the W $4f_{7/2}$ ($W^{(0)}$) peaks is 6.3 eV to be compared with the one of 6.1 eV for WC600. This difference measured on different authentic samples of tungsten metal, W_2C and WC is reported in Table II. It becomes higher on going from the metallic to the monocarbide tungsten (5.8–5.9 to 6.4). So the value obtained for WC830 indicated evidence of a decarburization of the tungsten carbide surface.

The C 1s spectrum of WC600 (Fig. 4a) is asymmetric (FWHM = 2.0 eV), the apparent maximum peaking at 285.5 eV. Considering the small shoulder at the lowest binding energy, we find a peak value of 283.2 (± 0.1 eV) [13] typical of a carbidic component in tungsten carbide. Besides this form, the C 1s signal shows different peaks attributed to polymeric carbon: C–C (285 eV), C–H (284.6 eV) and oxidized carbons towards high binding energies: C–O (285.9 eV) and C = O (287.9 eV) [14]. Fig. 4b shows the C 1s spectrum of WC830. The signal is large

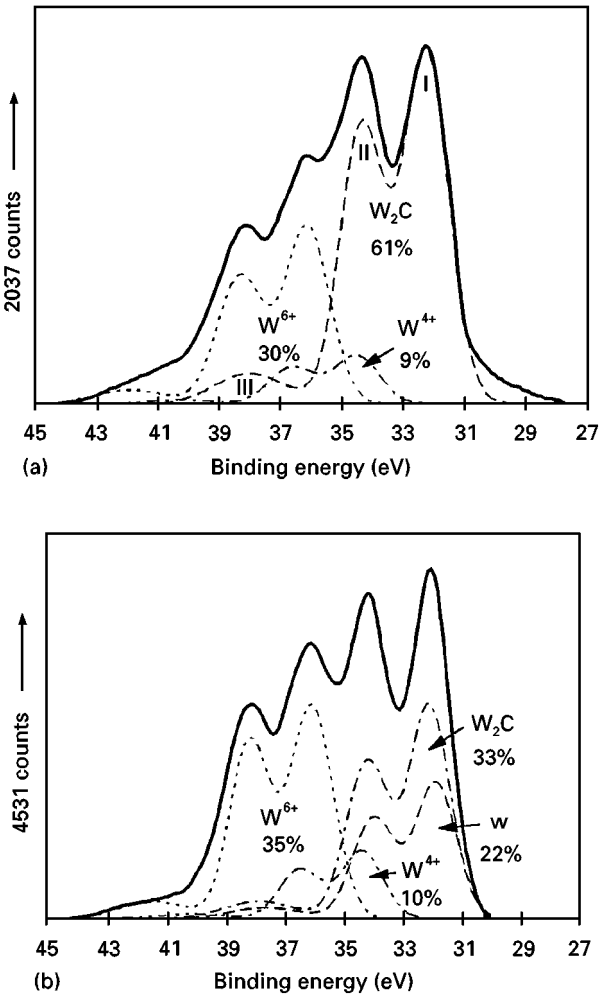

Figure 3 W4f XPS peaks after decomposition of $Cp_2W_2(CO)_4$(dmad) under hydrogen (a) at 600 °C for 2 h and (b) at 830 °C for 1 h. The photoelectron peaks W $4f_{7/2}$, W $4f_{5/2}$, tungsten satellite, are labelled 1, 2 and 3, for example, for the tungsten carbide component.

TABLE II Binding energies for tungsten and tungsten carbides species

Samples	Binding energies of the W $4f_{7/2}$ component (eV)	WO_3/W_t (%)	W $4f_{5/2}$ WO_3–W $4f_{7/2}$ W species (%)
W metal (sheet)[a]	31.8[e]	> 40	6.35
W metal (powder)[b]	31.8[f]	> 40	6.4
	31.8[e]		
W metal (powder)[c]	31.8[f]	> 40	6.4
	31.8[e]		
W_2C (powder)[d]	32.1	39	6.1
WC (powder)	32.3[f]	47	5.8–5.9

[a]From Goodfellow, purity 99.95%.
[b]Prolabo 99.9%.
[c]Fluka, quality > 99.5%.
[d]This study.
[e]W $4f_{5/2}WO_3$ as reference; BE, 38.2 eV.
[f]C 1s as reference; BE, 285 eV.

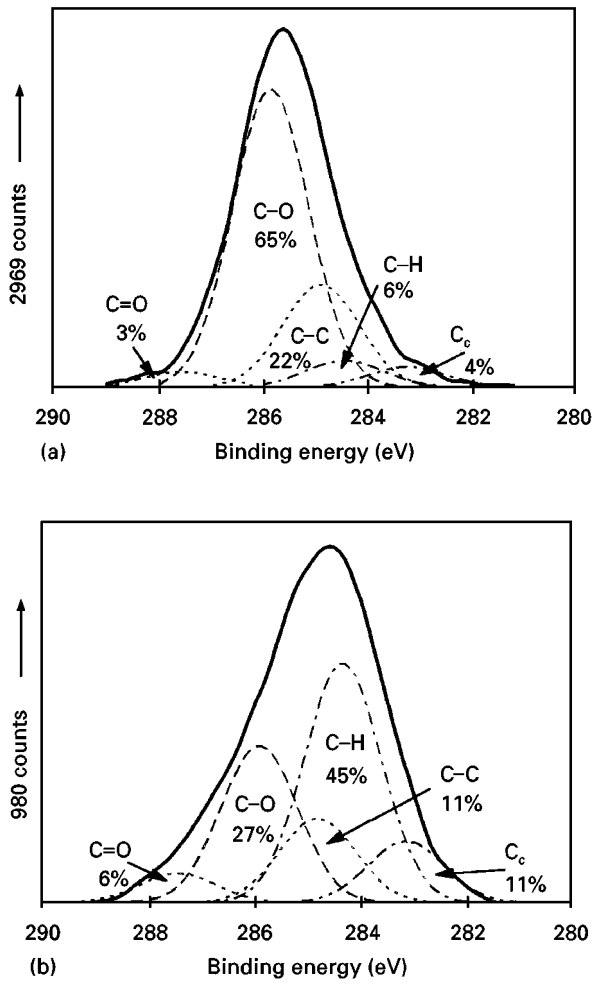

Figure 4 C 1s XPS peaks after decomposition of $Cp_2W_2(CO)_4$(dmad) under hydrogen (a) at 600 °C for 2 h and (b) at 830 °C for 1 h.

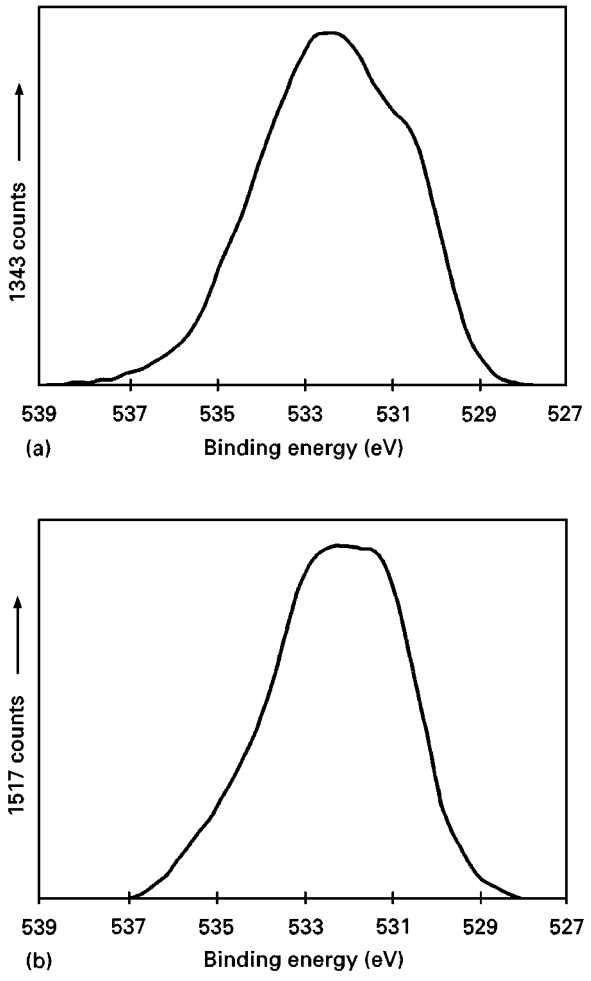

Figure 5 O 1s XPS peaks after decomposition of $Cp_2W_2(CO)_4$(dmad) under hydrogen (a) at 600 °C for 2 h and (b) at 830 °C for 1 h.

(FWHM = 2.2 eV), the apparent maximum being translated to weaker binding energies (284.8 eV). It shows the same different functionalities as above but with different atomic percentages (see Table III). The increase of the carbidic phase at the expense of the oxidized carbon component at 285.9 eV is noticeable.

The O 1s photoelectron peaks with maxima at 532.4 and 532 eV are broad for WC600 (FWHM = 4.3 eV) and WC830 (FWHM = 3.7 eV), respectively. Besides the component centred at ~531 eV, characteristic of the oxygen of transition metal oxides, at the low binding energy end of the spectrum, we notice high O 1s contributions due to oxygen linked to carbon (Fig. 5).

Quantitative determination of the average composition of the layer analysed by XPS was carried out using the procedure detailed in Section 2. The results are listed in Table III. The atomic ratio C_c/W_c for WC600 gives a value of 0.5, in perfect accordance with a W_2C stoichiometry. Based on this result and on the remarks stated above, we can envision a sub-stoichiometric $WC_{1-x}(0 < x < 0.5)$ surface state for WC830 or a mixture of W_2C and tungsten metal. From these two possibilities, the second is supported by the XRD results.

The atomic ratios of total carbon and oxygen to tungsten ($C_t/W_t = 8.2$), ($O_t/W_t = 3.6$) indicate an extensive contamination of the sample WC600 by C–H–O polymeric species formed during the passivation step and the decomposition process which partially cover the carbidic sites. A substantial tungsten oxide contribution ($W_{ox} = 39\%$) generated by contacting tungsten carbide with a 2% O_2/N_2 mixture, is also observed. It should be stressed that carbon and oxygen remain as impurities mainly at the surface of the material. This is clearly evidenced by comparing the

TABLE III XPS surface composition of samples WC600 and WC830. W_c, carbidic tungsten, W_{ox}, oxydized tungsten, C_c, carbidic carbon, C_t, total carbon, C_{ox}, oxidized carbon, C, free carbon

Samples	W_c (%)	W (%)	W_{ox} (%)	W^{5+} W_{ox} (%)	$C_c W_c$	$C_t W_t$	$O_t W_t$	$C_c W_t$ (%)	$C_{ox} C_t$ (%$\sqrt{}$)	$C_f C_t$ (%)
WC600	61	0	39	23	0.5	8.2	3.6	4	67	28
WC830	33	22	45	22	0.3	1.6	1.7	10	32	55

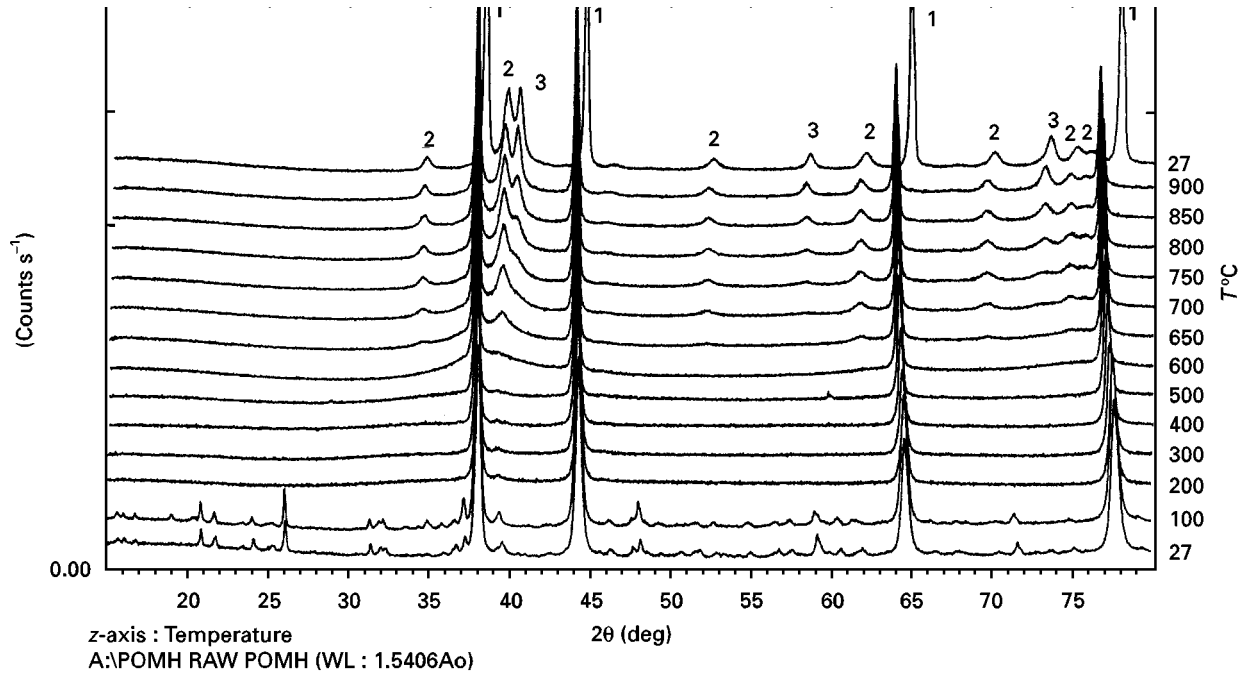

Figure 6 X-ray diffraction patterns during the *in situ* temperature-programmed decomposition of $Cp_2W_2(CO)_4$(dmad) under hydrogen from room temperature to 900 °C. 1, Au; 2, W_2C; 3, W.

XPS and elemental analysis results which lead to the formula $WC_{1.9}O_{0.2}H_{0.4}$ for WC600.

However, in the case of WC830, the C_t/W_t and O_t/W_t values of, respectively 1.6 and 1.7, are dramatically lowered, which shows the cleaning efficiency of hydrogen on these impurities at such a temperature. As a consequence of the minimization of these impurities deposits, oxygen diffuses to a higher extent during the passivation, and the surface of the material is more oxidized ($W_{ox}/W_t = 0.45$ against 0.39 for WC600).

In order to obtain additional information concerning the lowest decomposition temperature of $Cp_2W_2(CO)_4$(dmad), a temperature-programmed X-ray diffraction experiment was performed with a few milligrams of the sample. The diffraction patterns are reported in Fig. 6. For better clarity, we have extracted those recorded at 600, 650, 800 and 900 °C (Fig. 7).

The XRD pattern of the organometallic species exhibits numerous peaks at ambient temperature. The four intense peaks (2θ of about 38.2°, 44.4°, 64.6°, 77.5°) are characteristic of the gold plate deposited on the platinum cell. At 200 °C, the XRD diagram exhibits no $Cp_2W_2(CO)_4$(dmad) peaks, in accordance with an amorphous state, corresponding to melting and to initiation of ligands loss. Increasing the temperature to 500 °C gives a similar diagram to that at 200 °C. At 600 °C, a broad line at $2\theta = 38°$ is detected which could be attributed to the most intense line of W_2C. Indeed, at 650 °C, the XRD diagram shows a pure W_2C phase. A crystallite size of 2 nm is determined by XRD line broadening. At 700 °C, in addition to W_2C, the presence of a tungsten metal phase is also observed. Increasing the temperature further leads to a sharpening of the lines and the tungsten metal phase increases at the expense of ditungsten carbide.

If the XRD *in situ* experiment confirms the TGA results that a too high temperature of treatment results in some decarburization of W_2C into metallic tungsten, the latter two apparently differ quantitatively. Thus, if a mixture of W_2C and tungsten metal is detected at 900 °C by XRD, in the *in situ* experiment only tungsten metal appears after the TGA experiment at 900 °C. This could be explained by the presence of some oxygen as an impurity in hydrogen in the TGA experiment which could have accelerated the rate of decarburization of tungsten dicarbide.

As in the case of $Cp_2Mo_2(CO)_4$(dmad) [6], the TGA profile of which is given in Fig. 2b, the decomposition of $Cp_2W_2(CO)_4$(dmad) under hydrogen appears rather complicated. Because of behaviour analogies between molybdenum and tungsten, a process of decomposition of general trends can be expected for the two complexes.

Based on very simple thermodynamic considerations which stipulate that η^5 ligands, such as cyclopentadienyle, have binding dissociation energies stronger than those of η^1 ligands, and that the strength of bindings metal ligand (M–L) increases for the transition metals from the first to the third row (Table IV), one can envision that the carbonyl ligands should be the first to be removed and that the onset of decomposition of the tungsten derivative will be carried out at higher temperatures than that of the molybdenum homologue.

A direct comparison of the decomposition processes of $Cp_2W_2(CO)_4$(dmad) and $Cp_2Mo_2(CO)_4$(dmad) [6] given by TGA (Fig. 2) under the same experimental conditions, shows indeed that the onset of decomposition appears at a higher temperature for the tungsten derivative (first peak maximum for the former is 210 °C, and for the latter 132 °C).

It is possible to calculate that the total amount of carbon detected by gas chromatography (GC) is 8.9 per mole of the tungsten complex, which is very close

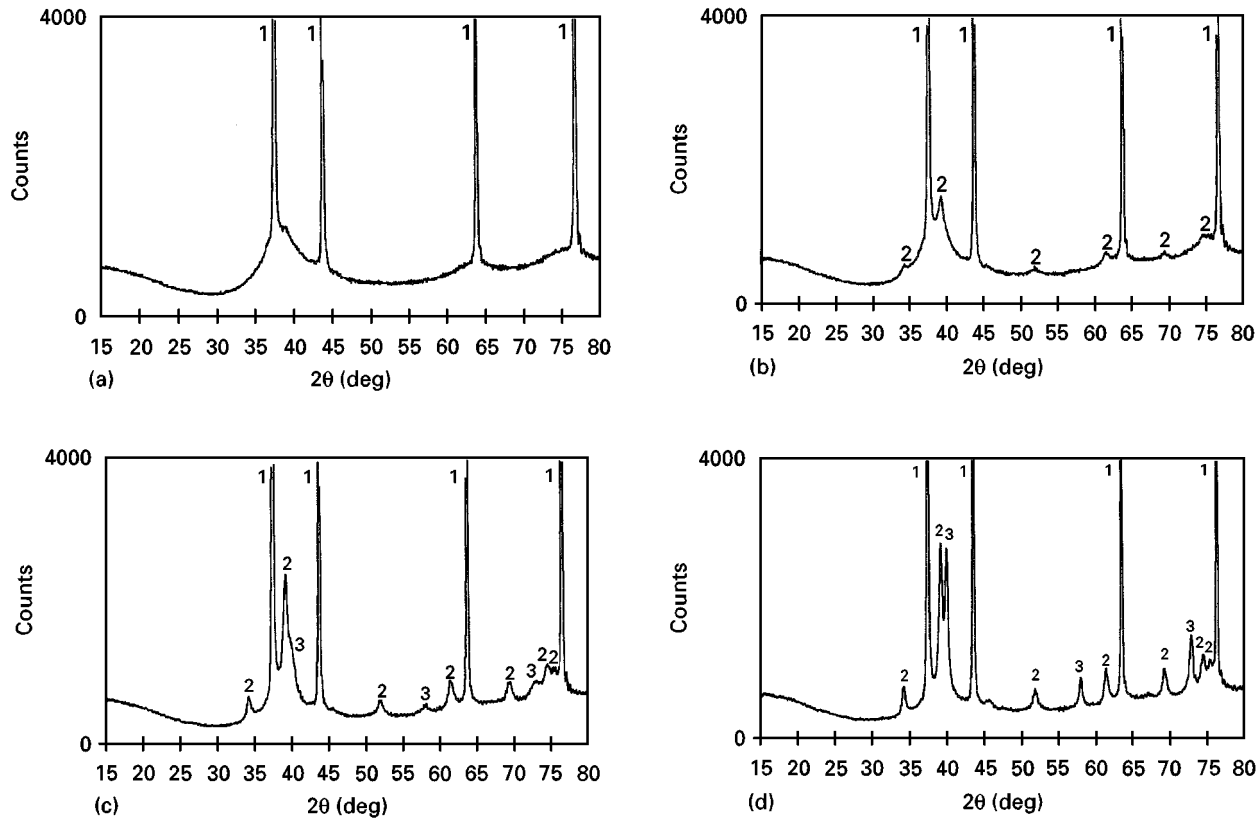

Figure 7 X-ray diffraction patterns during the *in situ* temperature-programmed X-ray diffraction decomposition of $Cp_2W_2(CO)_4$(dmad) under hydrogen at (a) 600 °C, (b) 650 °C, (c) 750 °C and (d) 900 °C. 1, Au; 2, W_2C; 3, W.

TABLE IV Bond dissociation energies (BDE) for organometallic compounds

Reactions	BDE (kcal mol^{-1})
$W(CO)_6 \rightarrow W(CO)_5 + CO$	46 ± 2 [15]
$Mo(CO)_6 \rightarrow Mo(CO)_5 + CO$	40 ± 2 [15]
$Cp_2Co(III)^+ \rightarrow CpCo(II)^+$	118 ± 10 [16]
$CpCo(II) \rightarrow CpCo(I)^+$	85 ± 10 [16]

to 9, taking into account the margin of error. This value is much lower than the total number of carbon atoms in 1 mole of the tungsten complex, which is 20. Hence, because TGA measurements and XRD diagrams of the solids obtained after a treatment at 650 °C have shown the formation of W_2C, it is clear that the removal of the cyclopentadienyl ligands is not detected by GC analysis, which only detects light elements. This shows that these ligands are removed without fragmentation and are not eluted from the GC column used here.

In the first step detected by GC, between 170 and 400 °C, in which evolution of CO, CO_2 and CH_4 occurs (Fig. 8a), four carbons are eliminated per mole of $Cp_2W_2(CO)_4$(dmad) (3.3 as CO, 0.42 as CO_2 and 0.29 as CH_4, Table V). As expected, production of CO appears first and the CO signal can be analysed as the superimposition of three signals: two narrow peaks at about 210 and 245 °C, and a very wide one between 210 and 400 °C (Fig. 8b). An attempt to estimate the areas of these three peaks gives numbers of carbon atoms per mole of the tungsten complex of about 1, 1 and 1.3, respectively, for the three contributions. The first narrow peaks very likely result from the elimination of two CO ligands, while the 1.3 CO, 0.42 CO_2 and 0.29 CH_4 are probably formed during the decomposition of one carbomethoxy group. The formation of CO_2 and CH_4 would occur simultaneously during CO_2CH_3 decomposition as

$$CO_2CH_3 + H_2 \rightarrow CO_2 + CH_4 \quad (2)$$

while the third contribution of CO would be formed by another CO_2CH_3 decomposition route, such as

$$CO_2CH_3 + H_2 \rightarrow CO + CH_3OH \quad (3)$$

CH_3OH, which has not been detected, would be transformed according to

$$CH_3OH + H_2 \rightarrow H_2O + CH_4 \quad (4)$$

$$CH_3OH \rightarrow CO + 2H_2 \quad (5)$$

These two CO_2CH_3 decomposition pathways were observed by the pyrolysis-mass spectrum of $Cp_2Mo_2(CO)_4$(dmad) in H_2–Ar flow (10/90) previously [6]. It should be noted that, while the elimination of the 2 CO ligands is very fast, that of CO_2CH_3 gives a broad contribution to the GC spectrum. In the second step, only the CH_4 formation (4.65 CH_4 per mole of the tungsten complex) and a very small production of CO (0.2 CO per mole of the tungsten complex) have been detected. This step can be considered as the overlapping of a wide signal with CO and CH_4 formation between 400 and 600 °C, the areas of which correspond to the elimination of about 1.9 C

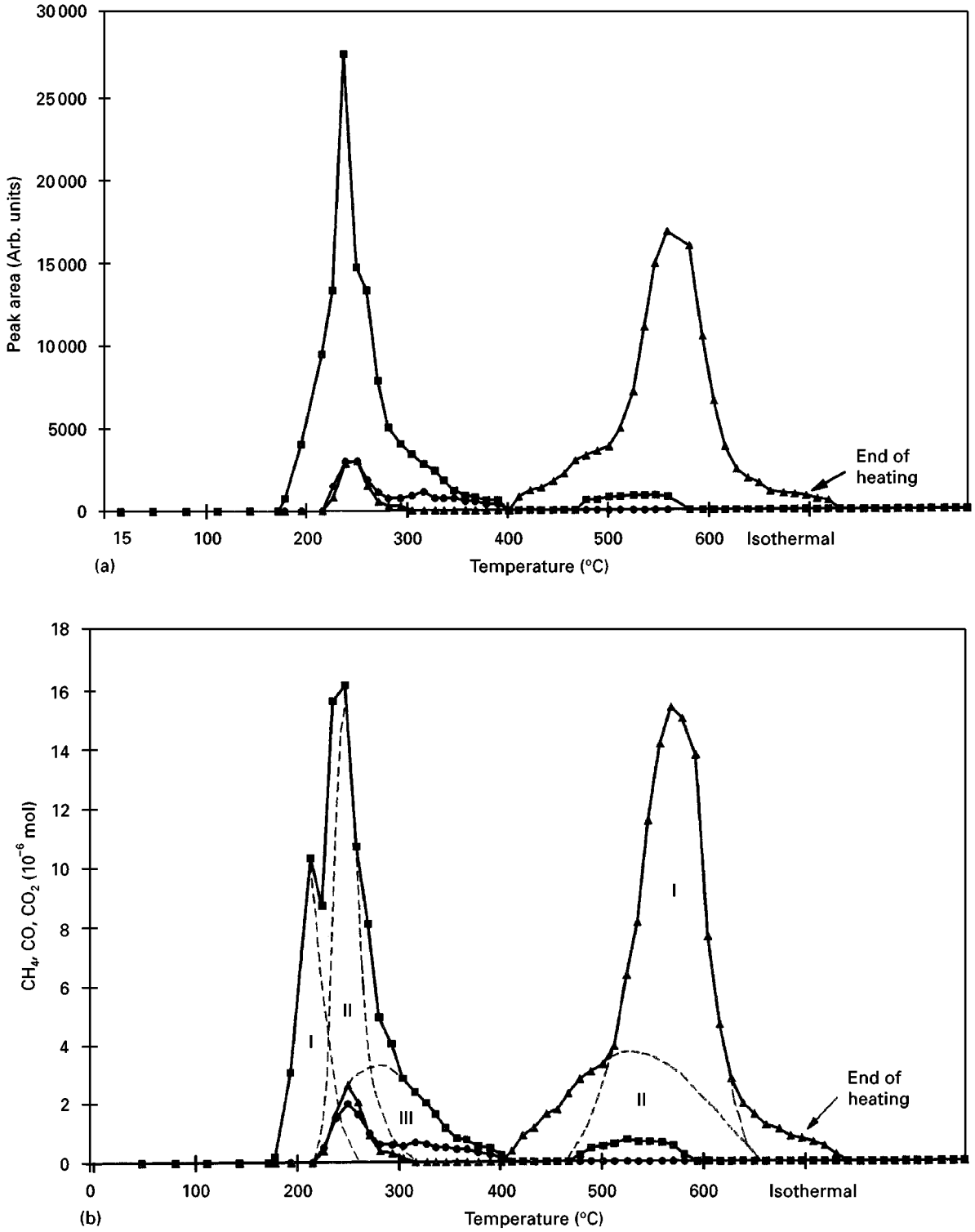

Figure 8 (a) Changes of (▲) CH_4 (■) CO and (●) CO_2 peak areas as a function of time and temperature during the decomposition process of $Cp_2W_2(CO)_4$(dmad) ($m = 21.6$ mg, d $H_2 = 50.9$ ml min^{-1}). (b) Evolution of the number of moles of (▲) CH_4, (■) CO and (●) CO_2 as a function of time and temperature.

atom, and a narrow one followed by a wide tail from about 500–600 °C forming only CH_4, corresponding to the elimination of 2.9 C, i.e. about 3 C atoms. Because the wide peak of the first step is likely to result from the elimination of one CO_2CH_3 fragment, the second wide peak probably arises from the elimination of the second CO_2CH_3 fragment, while the narrow peak and the tail at 600 °C correspond, respectively, to the removal of the two last CO ligands and of one carbon atom. It is interesting to notice that, in the second step, starting at 400 °C, all the fragments are eliminated mainly as CH_4, which indicates that CO, CO_2 and CH_3OH that can be found in the decomposition of CO_2CH_3 and CO of the ligands are reduced into CH_4. This probably reveals the hydrogenating catalytic properties of the tungsten component after two CO and a CO_2CH_3 fragment have been eliminated.

It is not easy to put together the results of TGA and of GC analysis because the sample weights were

TABLE V Number of moles of CO, CO_2, CH_4 produced during the decomposition of $Cp_2W_2(CO)_4$ (dmad) under hydrogen at 600 °C (21.6 mg min^{-1}, 50.9 ml min^{-1}, 1 h at 600 °C, 100 °C h^{-1})

Temp. range (°C)	nCO	nCO_2	nCH_4
170–400	3.3 I : 1; II : 1, III : 1.3	0.42	0.29
400–600	0.2	0	4.8 I : 2.9; II : 1.9

different, 8.1 and 21.6 mg, respectively; thus, with the same temperature gradient, one can expect that the various decomposition steps will be shifted towards higher temperatures in the second experiment. However, a close examination of the TGA curve indicates that at least six steps arise with different slopes from 100–210, 210–310, 310 to 360–370, 370–420, 420–550 and 550–600 °C. The temperature ranges corresponding to the removal of the various ligands overlap; nevertheless, it can be proposed that these steps could correspond, respectively, to the elimination of:

1. two CO and a part of one CO_2CH_3 and of one C_5H_5;
2. the remainder of the first CO_2CH_3 and of C_5H_5;
3. one C_5H_5 and part of the second CO_2CH_3;

4/5. the remainder of the second CO_2CH_3 and the two last CO and one C;

6. one C atom.

4. Conclusion

Our results show that it is possible to generate W_2C from $Cp_2W_2(CO)_4$(dmad) under hydrogen without the need for any carbiding gas. A temperature of 600 °C allowed us to recover a pure, hexagonal, closed-packed W_2C phase (XRD), compared with a temperature of 750 °C obtained for the decomposition of the organometallic complex under nitrogen reported by Laine and Hirschon [2].

Acknowledgements

We thank Mrs Guelton for performing the thermogravimetric analysis, and Mrs Burylo for performing the X-ray diffraction studies. We are also grateful to Doctor L. Gengembre for assistance in XPS analysis and Mr Briat for ^1H NMR analysis.

References

1. R. LAINE and A. HIRSCHON, in "Better Ceramics Through Chemistry II", edited by C. J. Brinker and D. E. Clark (Materials Research, New York, 1984) p. 373.
2. *Idem*, NATO ASI Series, Ser. E (1988) p. 21.
3. Z. XUE, K. G. CAULTON and M. H. CHISTOLM, *Chem. Mater.* **3** (1991) 384.
4. D. ZENG and M. J. HAMPDEN-SMITH, *ibid.* **4** (1992) 968.
5. L. E. TOTH, in "Transition Metal Carbides and Nitrides", edited by J. L. Margrave (Academic Press, New York, 1971) p. 10.
6. J. M. GIRAUDON, L. LECLERCQ, G. LECLERCQ, A. LÖFBERG and A. FRENNET, *J. Mater. Sci.* **28** (1993) 2449.
7. T. S. PIPER and G. WILKINSON, *J. Inorg. Nucl. Chem.* **3** (1956) 104.
8. R. LAINE and P. C. FORD, *J. Organometal. Chem.* **124** (1977) 29.
9. M. B. WARD, M. J. LIN and J. H. LUNSFORD, *J. Catal.* **50** (1977) 306.
10. T. E. MADEY, J. T. YATES and N. E. ERIKSON, *Surf. Sci.* **43** (1974) 526.
11. J. FIEDOR, A. PROCTOR, M. HOUALLA and D. M. HERCULES, *Surf. Interface Anal.* **23** (1995) 204.
12. P. BILOEN and G. T. POTT, *J. Catal.* **30** (1973) 169.
13. H. P. BONZEL and H. J. KREBS, *Surf. Sci.* **91** (1980) 489.
14. E. C. ONNYIRIUKA, *Chem. Mater.* **5** (1993) 798.
15. K. LEWIS, D. M. GOLDEN and G. P. SMITH, *J. Am. Chem. Soc.* **106** (1984) 3905.
16. D. B. JACOBSEN and B. S. FREISER, *ibid.* **107** (1985) 7400.

Received 19 April 1996
and accepted 18 April 1997